Relic gravitational waves in the frame of slow-roll inflation with a power-law potential and the detection

Minglei Tong*

National Time Service Center, Chinese Academy of Sciences, Xi'an, Shaanxi 710600, China and Key Laboratory of Time and Frequency Primary Standards, Chinese Academy of Sciences, Xi'an, Shaanxi 710600, China

We obtained the analytic solutions of relic gravitational waves (RGWs) for the slow-roll inflation with a power-law form potential of the scalar field, $V = \lambda\phi^n$. Based on a reasonable range of n constrained by cosmic microwave background (CMB) observations, we give tight constraints of the tensor-to-scalar ratio r and the inflation expansion index β for the fixed scalar spectral index n_s. Even though, the spectrum of RGWs in low frequencies is hardly depends on any parameters, the high frequency parts will be affected by several parameters, such as n_s, the reheating temperature $T_{\rm RH}$ and the index β_s describing the expansion from the end of inflation to the reheating process. We analyzed in detail all the factors which would affect the spectrum of RGWs in high frequencies including the quantum normalization. We found that the future GW detectors SKA, eLISA, BBO and DECIGO are promising to catch the signals of RGWs. Furthermore, BBO and DECIGO have the potential not only to distinguish the spectra with different parameters but also to examine the validity of the quantum normalization.

PACS number: 04.30.-w, 98.80.Es, 98.80.Cq

I. INTRODUCTION

The validity of general relativity and quantum mechanics make sure the generation of a stochastic background of relic gravitational waves (RGWs) [1–6] during the early inflationary stage, whose primordial amplitude could be determined by the quantum normalization at the time of the wave modes crossing the horizon during the inflation. Since the interaction of RGWs with other cosmic components is very weak, the evolution of RGWs are mainly determined by the behavior of cosmic expansion including the current acceleration [7, 8]. Therefore, RGWs could serve as an unique tool to study the very early Universe earlier than the recombination stage when the cosmic microwave background (CMB) radiation was generated. As an interesting source for gravitational wave (GW) detectors, RGWs exist everywhere and anytime unlike GWs radiated by usual astrophysical process. Moreover, RGWs spread a very broad range of frequency, $10^{-18}-10^{10}$ Hz, making themselves become one of the major scientific goals of various GW detectors with different response frequency bands. The current and planed GW detectors contain the ground-based interferometers, such as LIGO [9], Advanced LIGO [10, 11], VIRGO [12, 13], GEO [14], KAGRA [15] and ET [16, 17] aiming at the frequency range 10^2-10^3 Hz; the space interferometers, such as the future eLISA/NGO [18, 19] which is sensitive in the frequency range $10^{-4}-10^{-1}$ Hz, BBO [20, 21] and DECIGO [22, 23] which both are sensitive in the frequency range $0.1-10$ Hz; and the pulsar timing array, such as PPTA [24, 25] and the planned SKA [26] with the frequency window $10^{-9}-10^{-6}$ Hz. Besides, there some potential very-high-frequency GW detectors, such as the waveguide detector [27], the proposed gaussian maser beam detector around GHz [28], and the 100 MHz detector with a pair of 75-cm baseline synchronous recycling interferometers [29]. Furthermore, the very low frequency portion of RGWs also contribute to the anisotropies and polarizations of CMB [30], yielding a magnetic type polarization of CMB as a distinguished signal of RGWs. WMAP [31–34], Planck [35], the ground-based ACTPol [36] and the proposed CMBpol [37] are of this type.

*Email: mltong@ntsc.ac.cn

The reheating temperature, $T_{\rm RH}$, carries rich information of the early Universe, and relates to the decay rate of the inflation as $T_{\rm RH} \propto \sqrt{\Gamma}$ [38, 39]. Recently, the temperature of the reheating, $T_{\rm RH}$, was evaluated [40] according to the CMB observations by WMAP 7 [34], combining with the slow-roll inflation scenarios. Furthermore, the resultant RGWs was studied in [41]. However, these pieces of work underwent the assumption of a fixed form of the potential of the scalar filed driven the slow-roll inflation, $V(\phi) = \frac{1}{2}m^2\phi^2$. In this paper, we study a more general case of $V(\phi) = \lambda\phi^n$ [42], where λ is constant. Moreover, we adopt the limitation $n < 2.1$ obtained from the spectrum of CMB [43]. For a non-fixed value of n, it is hard to evaluate the temperature of the reheating process, $T_{\rm RH}$, using the method employed in [40]. Thus, we choose several values of $T_{\rm RH}$ lying in the range of $\sim 10^4 - 10^8$ GeV, where the lower limit and the upper limit of $T_{\rm RH}$ are obtained from the constraints in [43] and [44], respectively. In the text, one will see that n and $T_{\rm RH}$ affect the increases of the scale factor in the early stages of the Universe. Once all the expansion histories of different stages are determined, the evolutions of the RGWs at various phases can be determined subsequently. For the present time, the solutions of RGWs can be obtained, whose different frequency bands correspond to the k-modes re-entered the horizon at different phases. On the other hand, the anisotropies due to the tensor metric perturbations (gravitational waves) can be scaled to those due to the observations of the scalar perturbations by introducing a parameter r called tensor-to-scalar ratio. Under the frame of the slow-roll inflation scenario, r will be constrained in a narrow range due to the constraints from n for a given value of the scalar spectral index n_s. Similarly, the inflation expansion index β will also be constrained in a narrow range. Besides, there is a simple relation between n and the preheating expansion index β_s describing the expansion behavior of the universe from the end of inflation to the reheating process. As will be shown below, the RGWs in the very high frequencies are sensitively dependent on the parameters n_s, β_s and $T_{\rm RH}$. Furthermore, the spectra of RGWs also depends on the condition of the quantum normalization. To this end, the spectra of RGWs given by different parameters and different conditions will confront the various current and planed GW detectors. The future detectors BBO and DECIGO are quite promising not only to determine various parameters but also to examine the validity of the quantum normalization.

Throughout this paper, we use the units $c = \hbar = k_B = 1$. Indices λ, μ, ν,... run from 0 to 3, and i, j, k,... run from 1 to 3.

II. RGWS IN THE ACCELERATING UNIVERSE

In a spatially flat universe, the existence of perturbations modifies the Friedmann-Robertson-Walker metric to be

$$ds^2 = a^2(\tau)[-d\tau^2 + (\delta_{ij} + h_{ij})dx^i dx^j], \tag{1}$$

where $a(\tau)$ is the scale factor, τ is the conformal time, and h_{ij} stands for the perturbations to the homogenous and isotropic spacetime background. In general, there are three kinds of perturbations: scalar perturbation, vectorial perturbation and tensorial perturbation. In this paper we only consider the tensorial perturbation, that is, gravitational waves. In the transverse-traceless (TT) gauge, h_{ij} satisfies: $\frac{\partial h_{ij}}{\partial x^j} = 0$ and $h^i{}_i = 0$, where we used the Einstein summation convention. In the Fourier k-modes space, it can be written as

$$h_{ij}(\tau, \mathbf{x}) = \sum_\sigma \int \frac{d^3k}{(2\pi)^{3/2}} \epsilon^{(\sigma)}_{ij} h^{(\sigma)}_k(\tau) e^{i\mathbf{k}\cdot\mathbf{x}}, \tag{2}$$

where $\sigma = +, \times$ stands for the two polarization states, the comoving wave number k is related with the wave vector $\mathbf{k}$ by $k = (\delta_{ij}k^i k^j)^{1/2}$, $h^{(\sigma)*}_{-k}(\tau) = h^{(\sigma)}_k(\tau)$ ensuring h_{ij} be real, and the polarization

tensor $\epsilon_{ij}^{(\sigma)}$ satisfies [2]:

$$\epsilon_{ij}^{(\sigma)}\epsilon^{(\sigma')ij}=2\delta_{\sigma\sigma'},\quad \epsilon_{ij}^{(\sigma)}\delta^{ij}=0,\quad \epsilon_{ij}^{(\sigma)}n^j=0,\quad \epsilon_{ij}^{(\sigma)}(-\mathbf{k})=\epsilon_{ij}^{(\sigma)}(\mathbf{k}). \tag{3}$$

In terms of the mode $h_k^{(\sigma)}$, the wave equation is

$$h_k^{(\sigma)\prime\prime}(\tau)+2\frac{a'(\tau)}{a(\tau)}h_k^{(\sigma)\prime}(\tau)+k^2h_k^{(\sigma)}(\tau)=0, \tag{4}$$

where a prime means taking derivative with respect to τ. The two polarizations of $h_k^{(\sigma)}(\tau)$ have the same statistical properties and give equal contributions to the unpolarized RGWs background, so the super index (σ) can be dropped. The approximate solutions of Eq. (4) are well analyzed in [2, 3, 7], and are detailed listed in [41] given an accelerating universe at present. Furthermore, the analytic solutions were also studied by many authors [8, 45–48]. For a power-law form of the scale factor $a(\tau)\propto\tau^\alpha$, the analytic solution to Eq.(4) is a linear combination of Bessel and Neumann functions

$$h_k(\tau)=\tau^{\frac{1}{2}-\alpha}\big[C_1J_{\alpha-\frac{1}{2}}(k\tau)+C_2N_{\alpha-\frac{1}{2}}(k\tau)\big], \tag{5}$$

where the constants C_1 and C_2 for each stage are determined by the continuities of $h_k(\tau)$ and $h'_k(\tau)$ at the joining points τ_1,τ_s,τ_2 and τ_E [8, 45]. Therefore, the all the constants in the solutions of RGWs can be completely fixed, once the initial condition is given. In a spatially flat $(k=0)$ universe, the scale factor indeed has a power-law form in various stages [2, 41, 45, 47]. It is described by the following successive stages :

The inflationary stage:

$$a(\tau)=l_0|\tau|^{1+\beta},\quad -\infty<\tau\le\tau_1, \tag{6}$$

where the inflation index β is an model parameter describing the expansion history during inflation. The special case of $\beta=-2$ corresponds the exact de Sitter expansion. However, both the model-predicted and the observed results indicate that the value of β could differ slightly from -2.

The preheating stage :

$$a(\tau)=a_z|\tau-\tau_p|^{1+\beta_s},\quad \tau_1\le\tau\le\tau_s, \tag{7}$$

where the parameter β_s describes the expansion behavior of the preheating stage from the end of inflation to the happening of reheating process followed by the radiation-dominant stage. In some literatures [41, 49], β_s is set to be 1 , however, we take β_s as a free parameter in the paper.

The radiation-dominant stage :

$$a(\tau)=a_e(\tau-\tau_e),\quad \tau_s\le\tau\le\tau_2. \tag{8}$$

The matter-dominant stage:

$$a(\tau)=a_m(\tau-\tau_m)^2,\quad \tau_2\le\tau\le\tau_E. \tag{9}$$

The accelerating stage up to the present time τ_0 [7]:

$$a(\tau)=l_H|\tau-\tau_a|^{-\gamma},\quad \tau_E\le\tau\le\tau_0, \tag{10}$$

where γ is a Ω_Λ-dependent parameter, and Ω_Λ is the energy density contrast. To be specific, we take $\gamma\simeq1.97$ [50] for $\Omega_\Lambda=0.73$ [34] in this paper. It is convenient to choose the normalization

$|\tau_0 - \tau_a| = 1$, i.e., the present scale factor $a(\tau_0) = l_H$. From the definition of the Hubble constant, one has $l_H = \gamma/H_0$, where $H_0 = 100\,h$ km s^{-1}Mpc^{-1} is the present Hubble constant. We take $h \simeq 0.704$ [34] throughout this paper. Supposing β and β_s are model parameters, all the constants included trough Eq.(6) to Eq. (10) can be fixed by the continuity of $a(\tau)$ and $a'(\tau)$ at the four given joining points τ_1, τ_s, τ_2 and τ_E, if one knows the increases of the scale factor of various stages, i.e., the definite values of $\zeta_1 \equiv a(\tau_s)/a(\tau_1)$, $\zeta_s \equiv a(\tau_2)/a(\tau_s)$, $\zeta_2 \equiv a(\tau_E)/a(\tau_2)$, and $\zeta_E \equiv a(\tau_0)/a(\tau_E)$.

The spectrum of RGWs $h(k,\tau)$ is defined by

$$\langle h^{ij}(\tau,\mathbf{x})h_{ij}(\tau,\mathbf{x})\rangle \equiv \int_0^\infty h^2(k,\tau)\frac{dk}{k}, \tag{11}$$

where the angle brackets mean ensemble average. The dimensionless spectrum $h(k,\tau)$ relates to the mode $h_k(\tau)$ as [47]

$$h(k,\tau) = \frac{\sqrt{2}}{\pi}k^{3/2}|h_k(\tau)|. \tag{12}$$

The one that we are of interest is the present RGWs spectrum $h(k,\tau_0)$. The characteristic comoving wave number at a certain joining time τ_x is give by [41]

$$k_x \equiv k(\tau_x) = \frac{2\pi a(\tau_x)}{1/H(\tau_x)}. \tag{13}$$

After a long but simple calculation, it is easily to obtain $k_H = 2\pi\gamma$ and the following relations:

$$\frac{k_E}{k_H} = \zeta_E^{-\frac{1}{\gamma}}, \quad \frac{k_2}{k_E} = \zeta_2^{\frac{1}{2}}, \quad \frac{k_s}{k_2} = \zeta_s, \quad \frac{k_1}{k_s} = \zeta_1^{\frac{1}{1+\beta_s}}. \tag{14}$$

In the present universe, the physical frequency relates to a comoving wave number k as

$$f = \frac{k}{2\pi a(\tau_0)} = \frac{k}{2\pi l_H}. \tag{15}$$

The present energy density contrast of RGWs defined by $\Omega_{GW} = \langle\rho_g\rangle/\rho_c$, where $\rho_g = \frac{1}{32\pi G}h_{ij,0}h^{ij}_{,0}$ is the energy density of RGWs and $\rho_c = 3H_0^2/8\pi G$ is the critical energy density, is given by [3, 5]

$$\Omega_{GW} = \int_{f_{low}}^{f_{upper}} \Omega_g(f)\frac{df}{f}, \tag{16}$$

with

$$\Omega_g(f) = \frac{2\pi^2}{3}h_c^2(f)\Big(\frac{f}{H_0}\Big)^2 \tag{17}$$

being the dimensionless energy density spectrum. We have used a new notation, $h_c(f) = h(f,\tau_0)/\sqrt{2}$, called *characteristic strain spectrum* [5] or *chirp amplitude* [51]. The lower and upper limit of integration in Eq.(16) can be taken to be $f_{low} \simeq f_E$ and $f_{upper} \simeq f_1$, respectively, since only the wavelength of the modes inside the horizon contribute to the total energy density.

III. THE INCREASES OF THE SCALE FACTOR

For the simple ΛCDM model, the late-time acceleration of the universe is well know. One easily has $\zeta_E = 1 + z_E = (\Omega_\Lambda/\Omega_m)^{1/3} \simeq 1.4$, where z_E is the redshift when the accelerating expansion

begins. The increase of the scale factor duration of the matter-dominated stage can also be obtained straightforwardly, $\zeta_2 = \frac{a(\tau_0)}{a(\tau_2)}\frac{a(\tau_E)}{a(\tau_0)} = (1+z_{eq})\zeta_E^{-1}$ with $z_{eq} = 3240$ [34]. However, the histories of the radiation-dominated stage and the preheating stage are not known well. Recently, Mielczarek [40] proposed a method to evaluate the reheating temperature, $T_{\rm RH}$, under the frame of the slow-roll inflation model with a quadratic potential $V(\phi) = \frac{1}{2}m^2\phi^2$ combing the observations from WMAP. Using this method, ζ_s and ζ_1 can be determined subsequently with the evaluation of $T_{\rm RH}$ [41]. In this paper, we consider a more general power-law form of the potential, $V(\phi) = \lambda\phi^n$, where λ is a constant. For this general form of $V(\phi)$, it is hard to obtain the analytic expression of the energy density of the universe at the end of inflation, and in turn, it is hard to obtain the temperature of reheating analytically. Hence, we will take some reasonable values of $T_{\rm RH}$ constrained by CMB observations[43].

Firstly, we discuss the value of ζ_s. After reheating, the universe is filled with the relativistic plasma, which undergoes a adiabatic expansion as long as the entropy transfer between the radiation and other components can be neglected. The adiabatic approximation leads to the conservation of the entropy, i.e., $dS = 0$. It implies sa^3 =const, where the entropy density s of radiation is given by

$$s = \frac{2\pi^2}{45} g_s T^3. \tag{18}$$

Here, g_s counts the effective number of relativistic species contributing to the radiation entropy. Another similar quantity g, counting the effective number of relativistic species contributing to the energy density of radiation, relates to energy density:

$$\rho = \frac{\pi^2}{30} g T^4. \tag{19}$$

The behavior of g and g_s with different energy scale were demonstrated in [46]. At the energy above ~ 0.1 MeV, one has $g = g_s$. Moreover, at the energy scales above ~ 1 TeV, $g = 106.75$ in the standard model, and $g \simeq 220$ in the minimal extension of supersymmetric standard model, respectively. On the other hand, at the energy scales below ~ 0.1 MeV, $g = 3.36$ and $g_s = 3.91$ respectively. According to the conservation of entropy, one can easily gets the increase of the scale factor from the reheating till the recombination [40],

$$\frac{a_{rec}}{a(\tau_s)} = \frac{T_{\rm RH}}{T_{rec}} \left(\frac{g_{*s}}{g_{\star s}}\right)^{1/3}, \tag{20}$$

where a_{rec} and T_{rec} stand for the scale factor and the temperature at the recombination, respectively. g_{*s} and $g_{\star s}$ count the effective number of relativistic species contributing to the entropy during the reheating and that during recombination, respectively. As discussed in [43], the lower band of the reheating energy scale is 17.3 TeV constrained by the observed scalar power spectrum of CMB at 95% of the confidence limit. Thus, in this paper we assume $g_{*s} \simeq 200$ eclectically, which was also employed in [43]. On the other hand, one has $g_{\star s} = 3.91$ including the contributions of the effective number from photons and three species of massless neutrinos to the radiation entropy during the recombination, since the energy scale at the recombination $T_{rec} = T_{\rm CMB}(1+z_{rec}) \sim 10^{-7}$ MeV. Under the assumption of $g_{*s} \simeq 200$, the lower bound of $T_{\rm RH} \gtrsim 6 \cdot 10^3$ GeV was obtained [43]. On the other hand, gravitinos production gives an upper bound [52]. For instance, in the framework of the Constrained minimal supersymmetric standard model [44], the upper bound of $T_{\rm RH}$ was found that $T_{\rm RH} \lesssim$ a few $\times 10^7$ GeV from over-production of ^{6}Li from bound state effects, and moreover, $T_{\rm RH}$ can be relaxed to $\lesssim$ a few $\times 10^8$ GeV when a more conservative bound on ^{6}Li/^{7}Li was used. However, if one does not consider the gravitinos production problem, the most upper bound of $T_{\rm RH}$

could be up to $\lesssim 3 \cdot 10^{15}$ GeV coming from the energy scale at the end of inflation [43]. Based on Eq. (20), one easily obtain

$$\zeta_s = \frac{a(\tau_2)}{a_{rec}} \frac{a_{rec}}{a(\tau_s)} = \frac{T_{\rm RH}}{T_{\rm CMB}(1+z_{eq})} \left(\frac{g_{*s}}{g_{\star s}}\right)^{1/3}, \tag{21}$$

where we have used $T_{rec} = T_{\rm CMB}(1+z_{rec})$. With $T_{\rm CMB} = 2.725$ K $= 2.348 \cdot 10^{-13}$ GeV [34], one has $\zeta_s \simeq 5 \times 10^{16}$ for example. Secondly, we discuss the evaluation of ζ_1. First of all, we briefly recall the slow-roll inflation model. For slow-roll inflation, the evolution is described by the usual slow-roll parameters [53]:

$$\epsilon \equiv \frac{m_{Pl}^2}{16\pi}\left(\frac{V'}{V}\right)^2, \qquad \eta \equiv \frac{m_{Pl}^2}{8\pi}\frac{V''}{V}, \tag{22}$$

which are required to be much small than unity for the slow-roll approximation to be valid. ϵ approaches to unity at the end of inflation. When the slow-roll conditions are satisfied, inflation continues keeping the Hubble rate nearly constant, and the primordial tensor power spectrum and the scalar power spectrum are respectively given as [48, 51]:

$$\Delta_h^2(k,\tau_*) \approx \frac{16}{\pi}\left(\frac{H_*}{m_{\rm Pl}}\right)^2, \tag{23}$$

$$\Delta_{\mathcal{R}}^2(k,\tau_*) \approx \frac{1}{\pi\epsilon}\left(\frac{H_*}{m_{\rm Pl}}\right)^2, \tag{24}$$

where H_* is the Hubble rate during inflation, and τ_* stands for the moment when the k-mode exits the horizon. On the other hand, based on the observations of CMB, the present scalar power spectrum can be expanded in power laws,

$$\Delta_h^2(k) = \Delta_h^2(k_0)\left(\frac{k}{k_0}\right)^{n_t}, \tag{25}$$

$$\Delta_{\mathcal{R}}^2(k) = \Delta_{\mathcal{R}}^2(k_0)\left(\frac{k}{k_0}\right)^{n_s-1}, \tag{26}$$

where $\Delta_h^2(k_0)$ and $\Delta_{\mathcal{R}}^2(k_0)$ are the power spectrum of the tensor perturbations and curvature perturbations evaluated at the pivot wave number $k_0^{\rm p} = k_0/a(\tau_0) = 0.002$ Mpc^{-1} [34], respectively. Furthermore, under the slow-roll approximation, at the pivot wave number k_0 the spectral parameters are given by [53]

$$n_t \simeq -2\epsilon, \tag{27}$$

$$n_s \simeq 1 - 6\epsilon + 2\eta, \tag{28}$$

In general, the spectral indices n_t and n_s are $k-$depedent, described by the running parameters $\alpha_t \equiv dn_t/d\ln k$ and $\alpha_s \equiv dn_s/d\ln k$, respectively [47, 53–55]. However, α_t and α_s are only second order small quantities. Moreover, if one uses the quantum normalization (see below) as the initial condition for the generation of RGWs, α_t should be exactly zero. On the other hand, as will be seen below, non-zero α_s would induce an n_s greater than 1, which make us difficult to evaluate the increase of the scale factor from the k_0 mode exiting the horizon during inflation to the end of inflation. Hence, in this paper we will simply set $\alpha_t = \alpha_s = 0$. Note that Even though the value of n_t is quite uncertain, n_s can be well constrained by CMB [34] or BAO [56]. The ratio of the primordial

tensor power spectrum to the scalar power spectrum is defined as [48, 51]

$$r \equiv \frac{\Delta_h^2(k,\tau_*)}{\Delta_{\mathcal{R}}^2(k,\tau_*)} = 16\epsilon, \tag{29}$$

based on Eqs.(23) and (24). Therefore, at the pivot number k_0, one has

$$r = \frac{\Delta_h^2(k_0,\tau_i)}{\Delta_{\mathcal{R}}^2(k_0,\tau_i)} \simeq \frac{\Delta_h^2(k_0)}{\Delta_{\mathcal{R}}^2(k_0)}, \tag{30}$$

where τ_i is the k_0-mode exit the horizon during inflation. The approximation of the second equation in Eq.(30) accounts for that the pivot k_0 wave mode reentered the horizon a little earlier than the present time, and then has suffered a decay. Therefore, the ratio $\Delta_h^2(k_0)/\Delta_{\mathcal{R}}^2(k_0)$ can not exactly reflect the true value of r given by its definition, however, the deviation would be expected to be less than $\sim 0.8\%$ [41]. Hence, we will use this approximation when confront with the CMB observations. Furthermore, under this approximation, one has a simple relation:

$$n_t = 2\beta + 4, \tag{31}$$

since the primordial spectrum of RGWs has a power-law form $\Delta(k_0) \simeq \Delta(k_0,\tau_i) \propto k^{2\beta+4}$ [41]. WMAP 7 Mean [34] fixed $\Delta_{\mathcal{R}}^2(k_0) \equiv A_s = (2.43 \pm 0.11)\cdot 10^{-9}$. Thus, the non-zero value of r implies the existence of gravitational wave background, which induced uniquely the B-mode polarization of CMB [57]. At present only observational constraints on r have been given [33, 34]. The upper bounds of r are recently constrained [34] as $r < 0.24$ by WMAP+BAO+H_0 and $r < 0.36$ by WMAP 7 only for $\alpha_s = 0$, and $r < 0.49$ for $\alpha_s \neq 0$ by both the combination of WMAP+BAO+H_0 and the WMAP 7 only, respectively. Furthermore, using a discrete, model-independent measure of the degree of fine-tuning required, if $0.95 \lesssim n_s < 0.98$, in accord with current measurements, the tensor-to-ratio satisfies $r \gtrsim 10^{-2}$ [58]. Therefore, one can normalize the RGWs at $k = k_0$ using Eq. (30), if r can be determined definitely.

As analyzed by Mielczarek [40], for the pivot wave number k_0^{p}, the total increase of the scale factor from the mode exit the horizon during inflation up to the present time can be evaluated as

$$\zeta_{\mathrm{tot}} \simeq \frac{H_*}{k_0^{\mathrm{p}}}. \tag{32}$$

Due to Eqs. (24) and (26), one has

$$\frac{1}{\pi\epsilon}\left(\frac{H_*}{m_{\mathrm{Pl}}}\right)^2 \approx \Delta_{\mathcal{R}}^2(k_0), \tag{33}$$

where the approximation $\Delta_{\mathcal{R}}^2(k_0) \approx \Delta_{\mathcal{R}}^2(k_0,\tau_i)$ was used. Taking the form $V(\phi) = \lambda\phi^n$, one can easily have a relation:

$$\epsilon = \frac{n(1-n_s)}{2(n+2)} \tag{34}$$

from Eqs. (22) and (28). Plugging Eqs. (33) and (34) into Eq. (32) gives

$$\zeta_{\mathrm{tot}} \simeq \frac{m_{\mathrm{Pl}}}{k_0^{\mathrm{p}}}\sqrt{\frac{\pi n}{2(n+2)}(1-n_s)\Delta_{\mathcal{R}}^2(k_0)}. \tag{35}$$

On the other hand, if we assume the universe did a quasi-de Sitter expansion($\beta \approx -2$), the increase of a scalar factor from the moment of k_0 mode exiting the horizon during inflation to the end of inflation is give by

$$\zeta_i = e^N, \tag{36}$$

where N is the e-folding number, which can be estimated as

$$N \simeq -\frac{8\pi}{m_{\rm Pl}^2}\int_{\phi_{obs}}^{0}\frac{V(\phi)}{V'(\phi)}d\phi. \tag{37}$$

Concretely, for $V(\phi)=\lambda\phi^n$, one can get

$$N \simeq \frac{n+2}{2(1-n_s)}, \tag{38}$$

with the help of Eqs. (22) and (28). So, if $n=2$, Eq.(38) reduces to the result shown in [40]. Plugging Eq. (38) into Eq. (36), and using the identity

$$\zeta_{\rm tot}=\zeta_i\zeta_1\zeta_s\zeta_2\zeta_E, \tag{39}$$

one can easily obtain the complete expression of ζ_1:

$$\zeta_1=\frac{m_{\rm Pl}}{k_0^{\rm p}}\left[\pi\Delta_{\mathcal{R}}^2(k_0)(1-n_s)\frac{n}{2(n+2)}\right]^{1/2}\frac{T_{\rm CMB}}{T_{\rm RH}}\left(\frac{g_{\star s}}{g_{*s}}\right)^{1/3}\exp\left[-\frac{n+2}{2(1-n_s)}\right]. \tag{40}$$

One can examine that, for $n=2$, the above expression reduces to Eq. (11) in Ref.[41] after using Eq.(7) in the same reference. In the following, let us see the reasonable range of the index n constrained by both theories and observations. As well known, at the end of inflation, the scalar field ϕ oscillates quickly around some point where $V(\phi)$ has a minimum. In the limit that the oscillation rate is much greater than Hubble expansion rate H, and ignoring the coupling between the scalar field ϕ and other components, it is found that [42] the scalar field oscillations behave like a fluid with $p=\bar{w}\rho$, where the average equation of state $\bar{w}$ depends on the form of the potential $V(\phi)$. For $V(\phi)=\lambda\phi^n$, one has

$$\bar{w}=\frac{n-2}{n+2} \tag{41}$$

and ρ decreases as $a^{-6n/(n+2)}$. In particular, $n=2$, one has $\bar{w}=0$ and $\rho\propto a^{-3}$, which imply a matter-dominant like expansion of the preheating stage [49]. Adding the consideration of the coupling between the scalar field and the resulting relativistic particle creation, Martin and Ringeval [43] verified the relation (41) using a numerical method, and it was found that the average $\bar{w}$ never deviates from zero exceeding 8%. From theoretical consideration, one should have $\bar{w}<1$ to satisfy the positivity energy conditions; while $\bar{w}>-1/3$ to make sure the inflation must stop and the preheating stage begins. Due to Eq. (41), the condition $-1/3<\bar{w}<1$ leads to $n>1$. On the other hand, Martin and Ringeval [43] firstly gave a constraint on n based on the CMB observations, $n<2.1$. Therefore, based on both the theories and observations, the index n is constrained to be

$$1<n<2.1. \tag{42}$$

Note that, there is a relation between n and β_s. According to the energy conservation equation and the Friedmann Equation,

$$\dot{\rho}+3\frac{\dot{a}}{a}\rho(1+\bar{w})=0, \tag{43}$$

$$\left(\frac{\dot{a}}{a}\right)^2=\frac{8\pi G}{3}\rho, \tag{44}$$

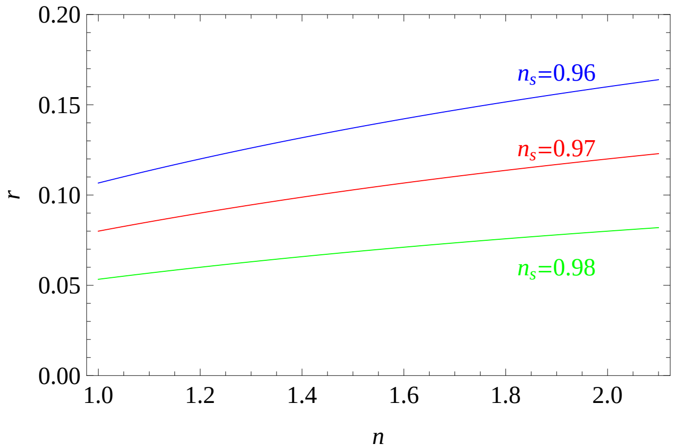

FIG. 1: The relation between r and n for the fixe value of $n_s = 0.96$, $n_s = 0.97$ and $n_s = 0.98$, respectively.

one can easily obtain $a \propto t^{2/(3+3\bar{w})} \propto \tau^{2/(1+3\bar{w})}$. Using Eqs. (7) and (41), and allowing for $\rho \propto a^{-6n/(n+2)}$, one has

$$\beta_s = \frac{4-n}{2(n-1)}. \tag{45}$$

Then, in principle, the expression of ζ_1 in Eq. (40) can be rewritten as a function of β_s. From the combination of Eqs. (42) and (45), one finds that, $n > 1$ leads to $\beta_s > -0.5$ and $n < 2.1$ leads to $\beta_s > 0.86$, respectively. Based on the range of n (or β_s) discussed above, we try to constrain some parameters combining with CMB observations.

IV. PARAMETERS CONSTRAINTS FROM OBSERVATIONS

As shown in the previous section, many parameters are dependent on the value of n_s. Seven-year WMAP Mean [34] gives $n_s = 0.967 \pm 0.014$, and $n_s = 0.982^{+0.020}_{-0.019}$ when one also considers the tensor mode contributions to the anisotropies of CMB. Moreover, the combination WMAP+BAO+H_0 Mean gives $n_s = 0.968 \pm 0.012$, and $n_s = 0.973 \pm 0.014$ when the tensor mode contributions are included. Independently, SDSS III predicts $n_s = 0.96 \pm 0.009$ [56]. As can be seen in Eq. (40), ζ is sensitively dependent on n_s, and in turn one can expect that the spectrum of RGWs also depend sensitively on n_s in the very high frequencies. Therefore, for a general demonstration, we consider the cases: $n_s = 0.96, 0.97$ and 0.98, respectively.

Firstly, let us constrain the tensor-to-scalar ratio r. According to Eqs. (22) and (29), it is straightly to get

$$r = \frac{8n}{n+2}(1-n_s). \tag{46}$$

We show this relation in Fig.1. One can see that r increases slowly with n. r lies in (0.11, 0.16), (0.08, 0.12), and (0.05, 0.08) for $n_s = 0.96$, $n_s = 0.97$, and $n_s = 0.98$, respectively. Similarly, from Eqs. (27) and (31), one has

$$\beta = -2 - \frac{n}{2(n+2)}(1-n_s), \tag{47}$$

which is shown in Fig.2. The parameter β is constrained in the range of $(-2.007, -2.010)$, $(-2.005, -2.008)$, and $(-2.003, -2.005)$ for $n_s = 0.96$, $n_s = 0.97$, and $n_s = 0.98$, respectively.

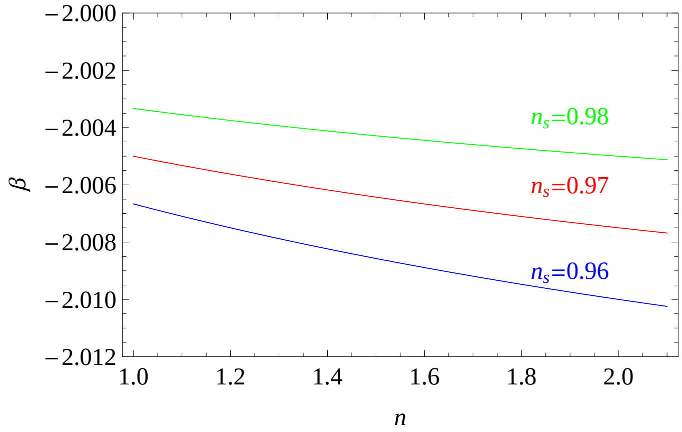

FIG. 2: The relation between β and n for the fixe value of $n_s = 0.96$, $n_s = 0.97$ and $n_s = 0.98$, respectively.

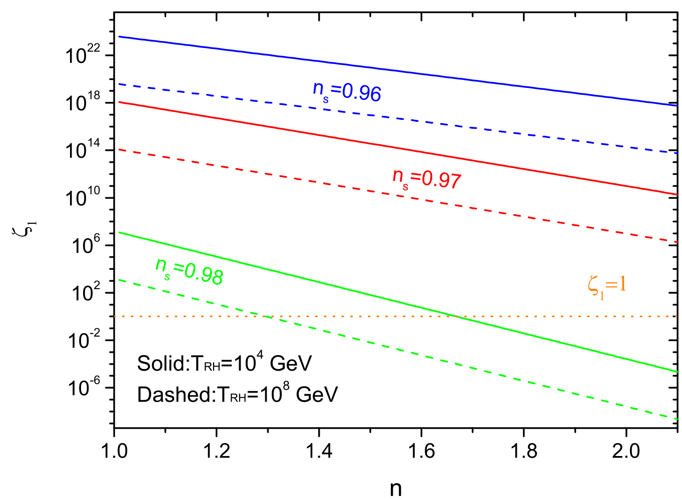

FIG. 3: ζ_1 as a function of n for the fixed value of $n_s = 0.96$, $n_s = 0.97$ and $n_s = 0.98$, respectively. The solid lines and dashed lines correspond to $T_{\rm RH} = 10^4$ GeV and $T_{\rm RH} = 10^8$ GeV, respectively. The dotted line represents $\zeta_1 = 1$.

Therefore, the range of n in Eq. (42) leads to very tight constraints on r and β, which are limited in very narrow ranges with definite value of n_s.

Now, let us see the increase of the scale factor during preheating stage ζ_1, which is expressed in Eq.(40). We plot it in Fig.3 as a function of n with definite values of $T_{\rm RH}$. Allowing for the expansion of the universe, one would expect that $\zeta_1 > 1$. As can be seen in Fig.3, the cases of $n_s = 0.96$ and 0.97 can make sure well the resultant ζ_1 being much larger than 1, however, the case of $n_s = 0.98$ can not be compatible with the fact $\zeta_1 > 1$ in the whole range of n shown in Eq.(42). If n_s is determined well to be as high as 0.98, it will give very tight constraints on n. Concretely, $n \lesssim 1.7$ and $n \lesssim 1.3$ for $T_{\rm RH} = 10^4$ GeV and $T_{\rm RH} = 10^8$ GeV, respectively. What we are more interesting are the characteristic frequencies given by Eq.(15). With the help of Eq. (14), one can easily get the characteristic frequencies: $f_H = H_0 \simeq 2.28 \cdot 10^{-18}$ Hz, $f_H = H_0 \simeq 2.28 \cdot 10^{-18}$ Hz, $f_E \simeq 1.93 \cdot 10^{-18}$ Hz, $f_2 \simeq 9.3 \cdot 10^{-17}$ Hz. The value of f_s depends linearly on $T_{\rm RH}$. For instance, $f_s \simeq 4.54 \cdot 10^{-3}$ Hz for $T_{\rm RH} = 10^4$ GeV and $f_s \simeq 45.4$ Hz for $T_{\rm RH} = 10^8$ GeV, respectively. Since $f_1 = f_s \zeta_1^{\frac{1}{1+\beta_s}}$, it depends on the values of n (or β_s), n_s and $T_{\rm RH}$. It is worth to be study in detail, since the characteristic

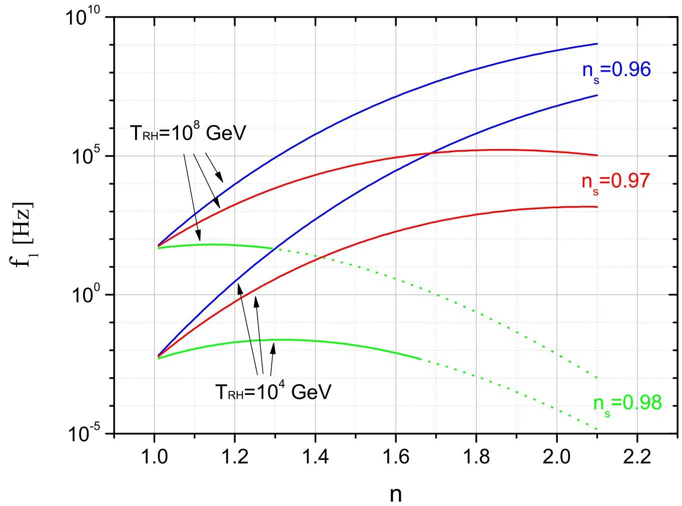

FIG. 4: The upper limit frequency f_1 as a function of n for different combinations of n_s and $T_{\rm RH}$. The dotted parts for $n_s = 0.98$ are constrained by the condition $\zeta_1 > 1$ shown in Fig. 3.

frequency f_1 is approximately the highest frequency of RGWs. The modes whose frequency higher than f_1 decay with the expansion of the universe [2, 3]. We plot f_1 as a function of n with definite n_s and $T_{\rm RH}$ in Fig.4. One can see that the behaviors of f_1 along with the increasing n are quite different for different values of n_s. For the case of $n_s = 0.98$, we plotted f_1 using dotted lines for the values of n constrained by $\zeta_1 > 1$ which are shown in Fig.3. In the part of large n, f_1 is larger for smaller values of n_s. On the other hand, in the limit of $n \to 1$, f_1 becomes a fixed value independent on n_s, and moreover, the asymptotic fixed f_1 is larger for a larger value of $T_{\rm RH}$. It is easy to understand if one has found that $\beta_s \to +\infty$ as $n \to 1$ from Eq.(45) which leads to $f_1 \to f_s$. The value of f_1 should be below the constraint from the rate of the primordial nucleosynthesis, $f_1 \lesssim 3 \times 10^{10}$ Hz [2]. When the acceleration epoch is considered, the constraint becomes $f_1 \simeq 4 \times 10^{10}$ Hz. This will in turn give some constraints on n, n_s and $T_{\rm RH}$.

As analyzed in our previous work [41], when the quantum normalization for the generation of RGWs during inflation is employed, one has

$$\Delta_{\mathcal{R}}(k_0) r^{1/2} = 8\sqrt{\pi} l_{Pl} H_0 \zeta_1^{\frac{\beta_s-\beta}{1+\beta_s}} \zeta_s^{-\beta} \zeta_2^{\frac{1-\beta}{2}} \zeta_E^{\frac{\beta-1}{\gamma}} \left(\frac{k_0}{k_H}\right)^{\beta}, \tag{48}$$

where $l_{Pl} = \sqrt{G}$ is the Planck length. In Eq.(48), there are totally six parameters: r, β, β_s, n, $T_{\rm RH}$ and n_s. However, among them only three are independent, due to Eqs.(45), (46) and (47). We show the $T_{\rm RH} - \beta$ relation with definite values of n_s in Fig.5. First of all, we define the range of $6 \cdot 10^3 - 10^8$ GeV as Region I; while the range of $6 \cdot 10^3 - 3 \cdot 10^{15}$ GeV as Region II. It is found that, under the condition of quantum normalization, $n_s = 0.96$ and $n_s = 0.98$ can be ruled out, since the resultant $T_{\rm RH}$ outside Region II. If one consider the gravitinos production problem, the case $n_s = 0.97$ would also be ruled out, since the resultant $T_{\rm RH}$ outside Region I. However, the resultant $T_{\rm RH}$ given by $n_s = 0.966$ lies well inside Region I for the whole range of β given by Eq. (47). Moreover, as shown in Fig.5, the quantum normalization will give a little tighter constraints on the range of β for $n_s = 0.967$ and $n_s = 0.968$. Note that, these results are based on the validity of quantum normalization, however, it is not the unique initial condition. Let us make a comparison with the previous results in [41]. Taking $n_s = 0.966$ for example, $n = 2$ leads to $T_{\rm RH} \simeq 3.4 \cdot 10^6$

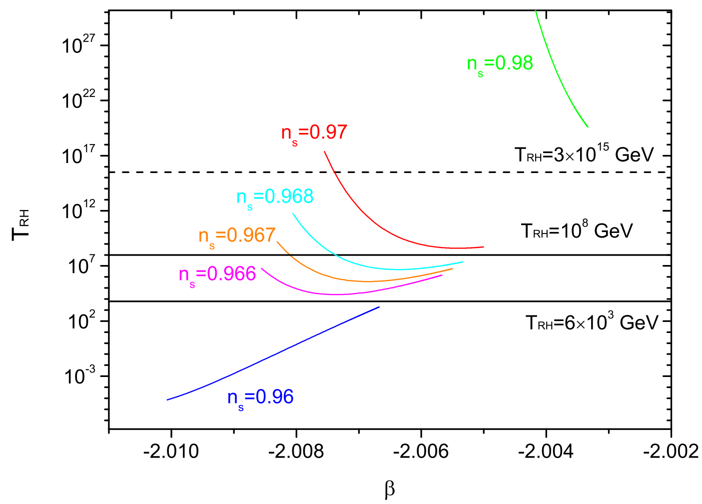

FIG. 5: The relation between $T_{\rm RH}$ and β based on Eq.(48) due to the condition of quantum normalization.

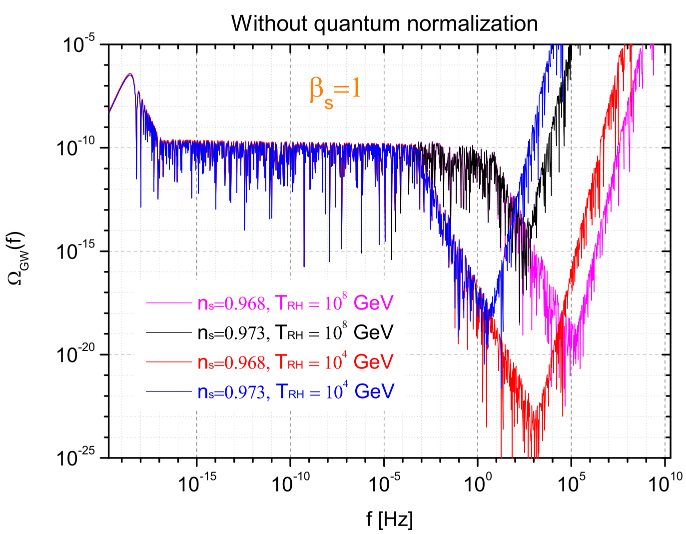

FIG. 6: The energy density spectra of RGWs for the fixed $\beta_s = 1$ with different combinations of n_s and $T_{\rm RH}$, without considering the quantum normalization.

GeV; while $T_{\rm RH} \simeq 2.8 \cdot 10^{12}$ GeV shown in Fig.1 in Ref.[41]. Hence, the discrepancy of $T_{\rm RH}$, at six orders of magnitude, indicates that the quantum normalization may be not a good initial condition. However, one should also keep in mind that we have used many approximations, which would also contribute a lot to the discrepancy of $T_{\rm RH}$ discussed above. Note that, if one does not consider quantum normalization, the zero point energy should be removed or else the cosmological constant would be 120 orders of magnitude larger than observed. Some effective methods [59] have been pointed out. In next section, we will demonstrate the spectra of RGWs with and without quantum normalization respectively.

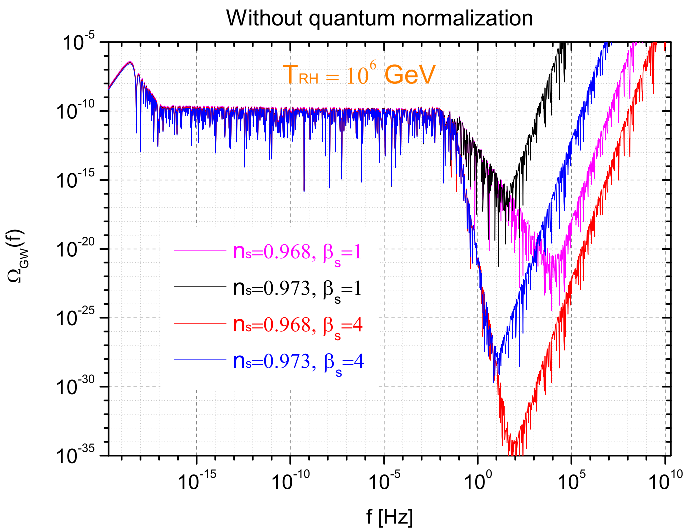

FIG. 7: The energy density spectra of RGWs for the fixed $T_{\rm RH} = 10^6$ GeV with different combinations of n_s and β_s, without considering the quantum normalization.

V. THE SPECTRA OF RGWS AND THEIR DETECTION

In this section, we demonstrate the energy density spectra of RGWs with reasonable values of the parameters and discuss the detection due to the current running and planned gravitational wave detectors.

As discussed in the previous sections, there are many parameters involved in the spectrum of RGWs. They are n_s, n, r, β, β_s, and $T_{\rm RH}$. However, among them only three are independent due to Eqs. (45)-(47). Furthermore, n_s has been constrained well from observations of CMB, BAO and H_0. Since the spectrum of RGWs in the high frequencies extreme sensitively depends on n_s, we discuss two cases of $n_s = 0.968$ and $n_s = 0.973$, respectively, based on the combination of WAMP+BAO+H_0 [34]. In the following, we regard β_s and $T_{\rm RH}$ as parameters, and choose some representative values of them since they have large uncertainties. In order to give a complete discussion, we will consider the spectra of RGWS both with and without quantum normalization. As analyzed in Sec.III, $T_{\rm RH}$ is constrained to be $T_{\rm RH} \sim 10^4 - 10^8$ GeV, and β_s is limited to be larger than 0.86. Firstly, let us see the case of no quantum normalization. Setting $\beta_s = 1$, Fig.6 shows the energy density spectra of RGWs, $\Omega_{\rm GW}(f)$, with different values of n_s and $T_{\rm RH}$. One can see that, all the $\Omega_{\rm GW}(f)$ nearly overlap each other in the low-frequencies. This is because the spectrum for $f \le f_s$ is only related to r and β [41], and, moreover, the differences of r and β are very small between the case $n_s = 0.968$ and the case $n_s = 0.973$ due to Eqs. (46) and (47). Explicitly, one has $r = 0.128, \beta = -2.008$ for $n_s = 0.968$ and $r = 0.108, \beta = -2.007$ for $n_s = 0.973$, respectively. However, in the part of high frequencies, $\Omega_{\rm GW}(f)$ exhibits different properties for different combinations of n_s and $T_{\rm RH}$. On one hand, for the same value of $T_{\rm RH}$, the spectrum $\Omega_{\rm GW}(f)$ with $n_s = 0.968$ and that with $n_s = 0.973$ have the same "turning point" from which $\Omega_{\rm GW}(f)$ decreases rapidly with the increasing frequency, and the "turning point" is just f_s which is only dependent on $T_{\rm RH}$. Moreover, the decreasing slope of the logarithm of the two spectra for $f \ge f_s$ are nearly the same since $\Omega_{\rm GW}(f) \propto f^{4+2\beta-2\beta_s}$ [41] which is reduced to $\Omega_{\rm GW}(f) \propto f^{-2}$ for $\beta \approx -2$ and $\beta_s = 1$. However, the $\Omega_{\rm GW}(f)$ with a smaller n_s has a larger upper limit frequency f_1 which responds to a lower amplitude of $\Omega_{\rm GW}(f)$. On the other hand, for the same value of n_s, the $\Omega_{\rm GW}(f)$ with a higher $T_{\rm RH}$ leads to not only a larger f_s

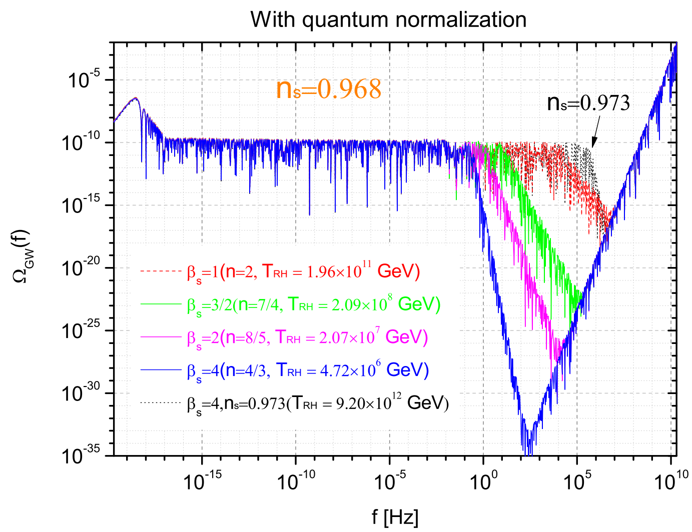

FIG. 8: The energy density spectra of RGWs under the condition of the quantum normalization.

but also a larger f_1 since $f_1 \propto T_{\rm RH}^{1/2}$ for $\beta_s = 1$ which can seen from the combination of Eqs. (14), (21) and (40). Fig.7 shows the energy density spectra of RGWs for the fixed value $T_{\rm RH} = 10^6$ GeV. One can see that a larger β_s leads to a steeper slope of the logarithm of $\Omega_{\rm GW}(f)$ and a smaller f_1 for the same values of n_s. In a word, $T_{\rm RH}$ determines the value of f_s, β_s determines the slope of the logarithm of $\Omega_{\rm GW}(f)$ for the fact that $\beta \approx -2$, and f_1 depends on all the three parameters especially n_s. Secondly, let us consider the case of the quantum normalization. Due to the resultant Eq. (48), among the three parameters $T_{\rm RH}$, β_s and n_s only two of them are independent. Taking n_s and $T_{\rm RH}$ as parameters, $\Omega_{\rm GW}(f)$ with some combinations of the two parameters are plotted in Fig.8.

Below, let us discuss the detection of RGWs using the ongoing and planned gravitational detectors which are sensitive at different frequency bands. As shown in Fig.6-Fig.8, the differences of the spectra of RGWs with different parameters are only significant in high frequency parts. Hence, we just take a characteristic combination of the parameters $n_s = 0.968$, $\beta_s = 1$ and $T_{\rm RH} = 10^6$ GeV for demonstration. As a conservative evaluation, in Fig. 9 we show the strain amplitudes, $h_c(f)/\sqrt{f}$ [5] of RGWs confronting the strain sensitivity curves of various gravitational wave detectors including the complete PPTA [25] and SKA [60] using the pulsar timing technique, and the space-based laser interferometers such as eLISA [19], BBO [20, 21], and the Fabry-Perot DECIGO [22]. One can see that, RGWs under the frame of the slow-roll inflation with a potential $V(\phi) \propto \phi^n$ are quite promising to be detected by the future SKA, eLISA, BBO and DECIGO. As seen from Fig.6-Fig.8, $\Omega_{\rm GW}(f)$ with different parameters have different properties in high frequencies. It would be interesting to discuss the detection of RGWs in high frequencies. In Fig. 10, we plot the characteristic amplitude of RGWs with different parameters and conditions compared to the instrumental noise, $\sqrt{fS_n(f)}$, of BBO, the ultimate DECIGO [23], the second generation ground-based laser interferometers AdvLIGO [11], and the third generation ET [17]. The parameters and conditions of RGWs are listed in Table I. $S_n(f)$ is the normal one-side noise spectrum of detectors. As can be seen in Fig.10, even though AdvLIGO and ET are hard to catch the signals of RGWs, BBO has the potential to distinguish RGWs with different parameters or different conditions in the frequency band $10^{-2} - 10^0$ Hz. Furthermore, the ultimate DECIGO has the capability to distinguish them more easily. Thus, the future BBO and DECIGO detections provide an important tool not only determining the parameters but also examining the validity of the quantum normalization when RGWs were generated during inflation. It

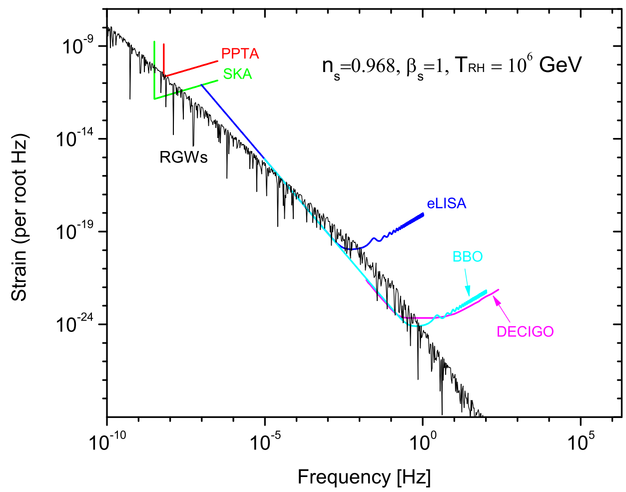

FIG. 9: The strain of RGWs with different parameters for $n_s = 0.968$, $\beta_s = 1$ and $T_{\rm RH} = 10^6$ GeV confronts against the current and planed GW detectors. The sensitivity curves of PPTA and SKA using pulsar timing technique are taken from Refs.[25] and [60], respectively. The curve of BBO is generated using the online "Sensitivity curve generator" [19] with the parameters in Table II of Ref.[20] and Table I of Ref.[21]. The curve of DECIGO is taken from Ref.[22].

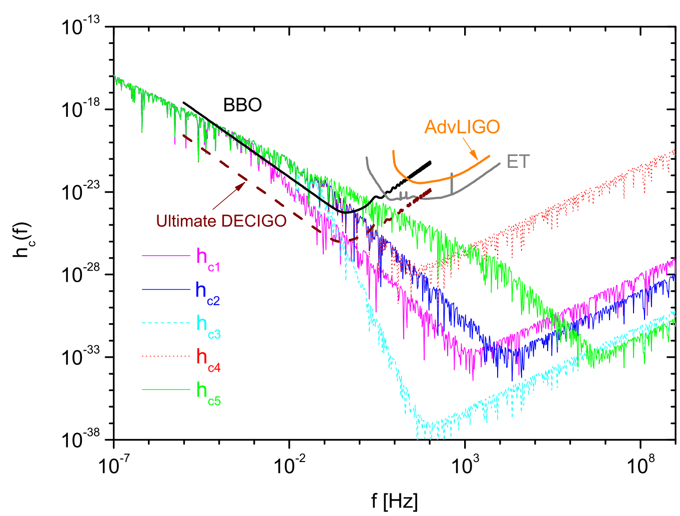

FIG. 10: The characteristic amplitude of RGWs in high frequencies confronting against the instrument noise $\sqrt{fS_n(f)}$ of BBO, Ultimate DECIGO [23], AdvLIGO and ET.

is worth to point out that, at frequencies lower than 10^{-2} Hz the signals of RGWs are contaminated by the confusion noise produced by galactic binaries [61]. Hence, we should focus on the frequencies higher than 10^{-2} in order to distinguish various spectra of RGWs.

VI. CONCLUSIONS AND DISCUSSIONS

In the frame of the slow-roll inflation with a power-law form $V = \lambda\phi^n$, we calculated the analytic solutions of RGWs. In the narrow range $1 < n < 2.1$, the tensor-to-scalar ratio r and the inflation

TABLE I: The definitions of h_c with different parameters. "N" stands for "No" meaning that the condition of the quantum normalization is not considered; while "Y" stands for "Yes" meaning that the condition of the quantum normalization is considered.

h_c	n_s	β_s	$T_{\rm RH}$	quantum normalization
h_{c1}	0.968	1	10^4 GeV	N
h_{c2}	0.968	1	10^6 GeV	N
h_{c3}	0.968	4	10^6 GeV	N
h_{c4}	0.973	1	10^6 GeV	N
h_{c5}	0.968	1	$2 \cdot 10^{11}$ GeV	Y

expansion index β are both tight limited to lie in narrow ranges for a given value of the scalar spectral index n_s. Concretely, r lies in (0.11, 0.16), (0.08, 0.12), and (0.05, 0.08) for $n_s = 0.96$, $n_s = 0.97$, and $n_s = 0.98$, respectively; while β lies in the range of $(-2.007, -2.010)$, $(-2.005, -2.008)$, and $(-2.003, -2.005)$ for $n_s = 0.96$, $n_s = 0.97$, and $n_s = 0.98$, respectively. Moreover, the preheating expansion index β_s is constrained to be $\beta_s > 0.86$. We found that the spectrum of RGWs in high frequencies depends on the parameters n_s, β_s and $T_{\rm RH}$. Explicitly, $T_{\rm RH}$ determines f_s where the flat RGWs spectrum decreases suddenly. β_s determines the decreasing slope of the logarithm of the spectrum. Whereas, the upper limit frequency f_1 is dependent on all the three parameters n_s, β_s and $T_{\rm RH}$. Besides, the quantum normalization for the generation of RGWs also affect the spectrum of RGWs in high frequencies.

Among the current and planed GW detectors, SKA using the pulsar timing technique and the space-based interferometers eLISA, BBO and DECIGO are promising to catch the signals of RGWs. Furthermore, BBO and DECIGO have the potential not only to distinguish the spectra with different parameters but also to examine the validity of the quantum normalization. Therefore, RGWs could become the most important tool to know the physics occurred in the very early Universe such as the inflation and reheating process. Even though we chose a series power-law form potential of the scalar field, as shown in [42], a polynomial form of the potential will be dominated by the lowest power of ϕ in V. In this case, the conclusion is not substantially modified. In our previous work [41], we got the $r - \beta$ relation for a particular potential $V = \frac{1}{2}m^2\phi^2$. However, for the more general case $V = \lambda\phi^n$, it is hard to obtain a complete analytic solution of $T_{\rm RH}$ and in turn the increases of the scale factor ζ_s and ζ_1. Therefore, in this paper, we set a series reasonable values of $T_{\rm RH}$ as additional parameters. The determination of n_s is very important, since it is sensitively affect our results. The future CMB experiments such as the Plank satellite [35], the ground-based ACTPol [36] and the planned CMBPol [37] will help us to determine the more convincible value of n_s. Therefore, one can expect accordingly that the spectrum of RGWs would be known better.

In principle, our analysis is valid for the slow-roll inflation with other forms of the potential $V(\phi)$. However, for some particular forms of $V(\phi)$, it would be difficult to get the analytic result of ζ_1 as a function of the parameters included in $V(\phi)$. Moreover, one could not effectively constrain the parameters in $V(\phi)$. However, one can still calculate ζ_1 numerically according to the whole calculating processes presented in Ref.[40], and then calculate the spectra of RGWs accordingly. More general inflationary models other than the slow-roll inflation and the slow-roll inflation with other forms of $V(\phi)$ would be studied in our future work.

ACKNOWLEDGMENT: This work is supported by the National Science Foundation of China

under Grant No. 11103024 and the program of the light in China's Western Region of CAS.

[1] L.P. Grishchuk, Sov.Phys.JETP **40**, 409 (1975); Class.Quant.Grav.**14**, 1445 (1997).
[2] L.P. Grishchuk, in *Lecture Notes in Physics*, Vol.562, p.167, Springer-Verlag, (2001), arXiv: gr-qc/0002035.
[3] L.P. Grishchuk, arXiv: gr-qc/0707.3319.
[4] A.A. Starobinsky, JEPT Lett. **30**, 682 (1979); Sov. Astron. Lett. **11**, 133 (1985);
V.A. Rubakov, M. Sazhin, and A. Veryaskin, Phys. Lett. B **115**, 189 (1982);
R. Fabbri and M.D. Pollock, Phys. Lett. B **125**, 445 (1983);
L. F. Abbott and M.B. Wise, Nucl. Phys. B **244**, 541 (1984);
B. Allen, Phys. Rev. D **37**, 2078 (1988);
V. Sahni, Phys. Rev. D **42**, 453 (1990);
H. Tashiro, T. Chiba, and M. Sasaki, Class. Quant. Grav. **21**, 1761 (2004);
A. B. Henriques, Class. Quant. Grav. **21**, 3057 (2004);
W. Zhao and Y. Zhang, Phys. Rev. D **74**, 043503 (2006).
[5] M. Maggiore, Phys. Rept. **331**, 283 (2000).
[6] M. Giovannini, PMC Phys. A **4**, 1 (2010).
[7] Y. Zhang *et al.*, Class. Quant. Grav. **22**, 1383 (2005);
[8] Y. Zhang *et al.*, Class. Quant. Grav.**23**, 3783 (2006).
[9] http://www.ligo.caltech.edu/.
[10] http://www.ligo.caltech.edu/advLIGO/.
[11] S. J. Waldman (the LIGO Scientific Collaboration), arXiv:1103.2728.
[12] A. Freise, *et al.*, Class. Quant. Grav. **22**, S869 (2005);
http://www.virgo.infn.it/.
[13] https://wwwcascina.virgo.infn.it/senscurve/.
[14] B. Willke, *et al.*, Class. Quant. Grav. **19**, 1377 (2002);
http://geo600.aei.mpg.de/;
http://www.geo600.uni-hannover.de/geocurves/.
P. Barriga, C. Zhao, and D.G. Blair, Gen. Relativ. Gravit. 37, 1609 (2005).
[15] K. Somiya, Class. Quantum Grav. **29**, 124007 (2012).
[16] M. Punturo et al., Class. Quantum Grav. **27**, 194002 (2010).
[17] S. Hild et al., Class. Quantum Grav. **28**, 094013 (2011).
[18] P. Amaro-Seoane et al, Class. Quantum Grav. **29, 124016** (2012); http://elisa-ngo.org/.
[19] http://www.srl.caltech.edu/˜ shane/sensitivity/.
[20] J. Crowder and N.J. Cornish, Phys. Rev. D, **72**, 083005 (2005).
[21] C. Cutler and J. Harms, Phys. Rev. D, **73**, 042001 (2006).
[22] S. Kawamura et al., Class. Quantum Grav. **23**, S125-S131 (2006).
[23] H. Kudoh, A. Taruya, T. Hiramatsu, and Y. Himemoto, Phys. Rev. D, **73**, 064006 (2006).
[24] G. Hobbs, Class. Quant. Grav. **25**, 114032 (2008); J. Phys. Conf. Ser. **122**, 012003 (2008);
R.N. Manchester, AIP Conf. Series. Proc. **983**, 584 (2008), arXiv:0710.5026; arXiv:1004.3602.
[25] F.A. Jenet, *et al.*, Astrophys. J. **653**, 1571 (2006).
[26] M. Kramer et al., New Astr. **48**, 993 (2004); www.skatelescope.org.
[27] A.M. Cruise, Class.Quant.Grav. **17**, 2525 (2000) ;
A.M. Cruise and R.M.J. Ingley, Class. Quant. Grav. **22**, S479 (2005); Class. Quant. Grav. **23**, 6185 (2006);
M.L. Tong and Y. Zhang, Chin. J. Astron. Astrophys. **8**, 314 (2008).
[28] F.Y. Li, M.X. Tang and D.P. Shi, Phys. Rev. D **67**, 104008 (2003);
F.Y. Li *et al.*, Eur. Phys. J. C **56**, 407 (2008);
M.L. Tong, Y. Zhang, and F.Y. Li, Phys. Rev. D **78**, 024041 (2008).
[29] T. Akutsu et al., Phys. Rev. Lett. **101**, 101101 (2008).
[30] M. Zaldarriaga and U. Seljak, Phys.Rev.D**55**, 1830 (1997);
M. Kamionkowski, A. Kosowsky, and A. Stebbins, Phys. Rev. D**55**, 7368 (1997);
B.G. Keating, P.T. Timbie, A. Polnarev, and J. Steinberger, Astrophys. J. **495**, 580 (1998);
J. R. Pritchard and M. Kamionkowski, Ann. Phys.(N.Y.) **318**, 2 (2005);
W. Zhao and Y. Zhang, Phys.Rev.D**74**, 083006 (2006);
T.Y Xia and Y. Zhang, Phys. Rev. D**78**, 123005 (2008); Phys. Rev. D**79**, 083002 (2009);
W. Zhao and D. Baskaran, Phys. Rev. D **79**, 083003 (2009).
[31] H.V. Peiris, *et al*, Astrophys. J. Suppl. **148**, 213 (2003).
D.N. Spergel, *et al*, Astrophys. J. Suppl. **148**, 175 (2003).
[32] D.N. Spergel, *et al*, Astrophys. J. Suppl. **170**, 377 (2007).
L. Page, *et al*, Astrophys.J.Suppl. **170**, 335 (2007).
[33] G. Hinshaw, *et al*, Astrophys. J. Suppl. **180**, 225 (2009);

J. Dunkley, *et al*, Astrophys. J. Suppl. **180**, 306 (2009).
[34] E. Komatsu, *et al*, Astrophys. J. Suppl. **192**, 18 (2011).
[35] Planck Collaboration, arXiv:astro-ph/0604069; http://www.rssd.esa.int/index.php?project=Planck.
[36] M.D. Niemack et al., Proc. SPIE, **7741**, 77411S (2010).
[37] J. Dunkley *et al.*, in *CMBPol Mission Concept Study: Prospects for Polarized Foreground Removal*, 1141, 222 (AIP, New York, 2009).
[38] E.W. Kolb and M.S. Turner, *The Early Universe*, (Addison-Wesley, Reading, MA, 1990).
[39] K. Nakayama, S. Saito, Y. Suwa, and J. Yokoyama, JCAP, **0806**, 020 (2008).
[40] J. Mielczarek, Phys. Rev. D **83**, 023502 (2011).
[41] M. Tong, Class. Quantum Grav. **29**, 155006 (2012).
[42] M.S. Turner, Phys. Rev. D 28, 1243 (1983).
[43] J. Martin and C. Ringeval, Phys. Rev. D **82**, 023511 (2010).
[44] S. Bailly, K.-Y. Choi, K. Jedamzik, and L. Roszkowski, J. High Energy Phys. 05, 103 (2009).
[45] H. X. Miao and Y. Zhang, Phys. Rev. D **75**, 104009 (2007).
[46] Y. Watanabe and E. Komatsu, Phys. Rev. D **73**, 123515 (2006).
[47] M.L. Tong, Y. Zhang, Phys. Rev. D **80**, 084022 (2009).
[48] S. Kuroyanagi, T. Chiba, and N. Sugiyama, Phys. Rev. D **79**, 103501 (2009).
[49] A.A. Starobinsky, Phys. Lett. B **91**, 99 (1980);
[50] Y. Zhang, M.L. Tong, and Z.W. Fu, Phys. Rev. D **81**, 101501(R), (2010).
[51] L.A. Boyle and P.J. Steinhardt, Phys. Rev. D **77**, 063504 (2008).
[52] M.Y. Khlopov and A.D. Linde, Phys. Lett. B 138, 265 (1984); C.F. Giudice, I. Tkachev and A. Riotto, J. High Energy Phys. 08, 009 (1999); M. Lemoine, Phys. Rev. D 60, 103522 (1999); A.L. Maroto and A. Mazumdar, Phys. Rev. Lett. 84, 1655 (2000); R. Kallosh, L. Kofman, A.D. Linde, and A. Van Proeyen, Phys. Rev. D 61, 103503 (2000); A. Buonanno, M. Lemoine, and K.A. Olive, Phys. Rev. D 62, 083513 (2000); E.J. Copeland and O. Seto, Phys. Rev. D 72, 023506 (2005); K. Jedamzik, Phys. Rev. D 74, 103509 (2006); M. Kawasaki, K. Kohri, T. Moroi, and A. Yotsuyanagi, Phys. Rev. D 78, 065011 (2008).
[53] A. R. Liddle and D. H. Lyth, Phys. Lett. B**291**, 391 (1992); Phys. Rep. **231**, 1 (1993); *Cosmological inflation and large-scale structure*, Cambridge University Press (2000).
[54] A. Kosowsky and M.S. Turner, Phys. Rev. D **52**, R1739 (1995).
[55] L.P. Grishchuk and M. Solokhin, Phys. Rev. D **43**, 2566, (1991).
[56] A.G. Sanchez et al, arXiv:1203.6616.
[57] M. Amarie, C. Hirata and U. Seljak, Phys. Rev. D **72**, 123006 (2005);
A. Amblard, A. Cooray and M. Kaplinghat, Phys. Rev. D **75**, 083508 (2007).
[58] L.A. Boyle, P.J. Steinhardt, and N. Turok, Phys. Rev. Lett. **96**, 111301 (2006).
[59] H.A. Borges and S. Carneiro, Gen. Relativ. Gravit. **37**, 1385 (2005); S. Carneiro, J. Phys. A **40**, 6841 (2007); M. Tong and H. Noh, Eur. Phys. J. C **71**, 1586 (2011).
[60] A. Sesana, A. Vecchio, and C.N. Colacino, Mon. Not. R. Astron. Soc. **390**, 192 (2008).
[61] J. Liu, Mon. Not. R. Astron. Soc. **400**, 1850 (2009); J. Liu, Z. Han, F. Zhang, and Y. Zhang, Astrophys. J. **719**, 1546 (2010); and references therein.